

Study of the singly charged Higgs in the economical 3-3-1 model at e^+e^- colliders

Dang Van Soa and Dao Le Thuy*

Department of Physics, Hanoi University of Education, Hanoi, Vietnam

(Dated: May 29, 2018)

The $SU(3)_C \otimes SU(3)_L \otimes U(1)_X$ gauge model with two Higgs triplets (the economical 3-3-1 model) are presented. This model predicts a new singly-charged Higgs bosons H_2^\pm , namely a scalar bilepton (a particle of lepton number 2) with mass proportional to the bilepton mass M_Y through the coefficient λ_4 . Pair production of H_2^\pm at high energy e^+e^- colliders with polarization of e^+ , e^- beams was studied in detail. Numerical evaluation shows that if Higgs mass is not too heavy and at high degree of polarization then the reaction can give observable cross section in future colliders. The reaction $e^+e^- \rightarrow H_2^- W^+$ is also examined. Based on the result, it shows that production cross sections of $H_2^- W^+$ are very small, much below pair production of H_2^\pm , so that the direct production of them is in general not expected to lead to easily observable signals in e^+e^- annihilation.

PACS numbers: 12.60.Fr, 14.80.Cp, 12.60.Cn, 14.80.Mz

I. INTRODUCTION

Recent neutrino experimental results [1] establish the fact that neutrinos have masses and the standard model (SM) must be extended. Among the beyond-SM extensions, the models based on the $SU(3)_C \otimes SU(3)_L \otimes U(1)_X$ (3-3-1) gauge group have some intriguing features: Firstly, they can give partial explanation of the generation number problem. Secondly, the third quark generation has to be different from the first two, so this leads to the possible explanation of why top quark is uncharacteristically heavy.

There are two main versions of the 3-3-1 models. In one of them [2] the three known left-handed lepton components for each generation are associated to three $SU(3)_L$ triplets as $(\nu_l, l, l^c)_L$, where l_L^c is related to the right-handed isospin singlet of the charged lepton l in the SM. The scalar sector of this model is quite complicated (three triplets and one sextet). In the variant model [3] three $SU(3)_L$ lepton triplets are of the form $(\nu_l, l, \nu_l^c)_L$, where ν_l^c is related to the right-handed component of the neutrino field ν_l (a model with right-handed neutrinos). The scalar sector of this model requires three Higgs triplets, therefore, hereafter we call this version the 3-3-1 model with three Higgs triplets (331RH3HT). It is interesting to note that, in the 331RH3HT, two Higgs triplets have the same $U(1)_X$ charge with two neutral components at their top and bottom. Allowing these neutral components vacuum expectation values (VEVs), we can reduce number of Higgs triplets to be two. Based on the results, the model with two higgs triplets, namely the *economical 3-3-1 model* was proposed recently [4]. This model contains very important advantage, namely: There is no new parameter, but it contains very simple Higgs sector, hence the significant number of free parameters is reduced. In the Higgs sector of this model there are four physical Higgs bosons. Two of them are neutral physical fields (H^0 and H_1^0), others are singly charged bosons H_2^\pm .

The Higgs boson plays an important role in the SM, it is responsible for generating the masses of all the elementary particles (leptons, quarks, and gauge bosons). The experimental detection of them will be great triumph of the electroweak interactions and will mark new stage in high energy physics. However, the mass of the Higgs boson is a free parameter [5]. The trilinear Higgs self-coupling can be measure directly in pair production of Higgs particle at hadron and high energy e^+e^- linear colliders [6, 7, 8, 9], or at photon colliders [10]. Interactions among the standard model gauge bosons and Higgs bosons in the economical 3-3-1 model were studied in detail in our early work [11]. The trilinear gauge boson couplings in the 3-3-1 models were presented in [12] and production of bileptons in high energy collisions was studied recently [13]. Discovery potential for doubly charged Higgs bosons and the possibility to detect the neutral Higgs boson in the minimal version at e^+e^- colliders was considered [14, 15]. Production of the Higgs bosons in the 331RH3HT at the CERN LHC has been done in Ref. [16].

The polarization of electron and positron beams gives a very effective means to control the effect of the SM processes on the experimental analyses. Beam polarization is also an indispensable tool for the identification and study of new

*Electronic address: dvsoa@assoc.iop.vast.ac.vn

particles and their interactions. In this paper we turn our attention to the future perspective experiment, namely the production of the singly charged Higgs in the economical 3-3-1 model at high energy collisions with polarization of e^+ , e^- beams. The rest of this paper is organized as follows: In Section II, we give a brief review of the economical 3-3-1 model. Section III represents a detail calculation for cross section of pair production H_2^\pm with polarization of e^+ , e^- beams. Pair production of $H_2^- W^+$ via ZZ' fusion is given in Sec. IV. We summarize our result and make conclusions in the last section - Sec. V.

II. A REVIEW OF THE ECONOMICAL 3-3-1 MODEL

The particle content in this model, which is anomaly free, is given as follows [4]

$$\psi_{aL} = (\nu_{aL}, l_{aL}, N_{aL})^T \sim (1, 3, -1/3), \quad l_{aR} \sim (1, 1, -1), \quad (1)$$

where $a = 1, 2, 3$ is a family index. Here the right-handed neutrino is denoted by $N_L \equiv (\nu_R)^c$.

$$\begin{aligned} Q_{1L} &= (u_1, d_1, U)_L^T \sim \left(3, \frac{1}{3}\right), & Q_{\alpha L} &= (d_\alpha, -u_\alpha, D_\alpha)_L^T \sim (3^*, 0), & \alpha &= 2, 3, \\ u_{aR} &\sim \left(1, \frac{2}{3}\right), & d_{aR} &\sim \left(1, -\frac{1}{3}\right), & U_R &\sim \left(1, \frac{2}{3}\right), & D_{\alpha R} &\sim \left(1, -\frac{1}{3}\right). \end{aligned} \quad (2)$$

Electric charges of the exotic quarks U and D_α are the same as of the usual quarks, i.e. $q_U = \frac{2}{3}$ and $q_{D_\alpha} = -\frac{1}{3}$. The $SU(3)_L \otimes U(1)_X$ gauge group is broken spontaneously via two steps. In the first step, it is embedded in that of the SM via a Higgs scalar triplet

$$\chi = (\chi_1^0, \chi_2^-, \chi_3^0)^T \sim \left(3, -\frac{1}{3}\right), \quad (3)$$

acquired with VEV given by

$$\langle \chi \rangle = \frac{1}{\sqrt{2}} (u, 0, \omega)^T. \quad (4)$$

In the last step, to embed the gauge group of the SM in $U(1)_Q$, another Higgs scalar triplet

$$\phi = (\phi_1^+, \phi_2^0, \phi_3^+)^T \sim \left(3, \frac{2}{3}\right), \quad (5)$$

is needed with the VEV as follows

$$\langle \phi \rangle = \frac{1}{\sqrt{2}} (0, v, 0)^T. \quad (6)$$

The Yukawa interactions which induce masses for the fermions can be written in the most general form as

$$\mathcal{L}_Y = (\mathcal{L}_Y^\chi + \mathcal{L}_Y^\phi) + \mathcal{L}_Y^{\text{mix}}, \quad (7)$$

where

$$\begin{aligned} (\mathcal{L}_Y^\chi + \mathcal{L}_Y^\phi) &= h'_{11} \bar{Q}_{1L} \chi U_R + h'_{\alpha\beta} \bar{Q}_{\alpha L} \chi^* D_{\beta R} \\ &\quad + h_{ij}^e \bar{\psi}_{iL} \phi e_{jR} + h_{ij}^\epsilon \epsilon_{pmn} (\bar{\psi}_{iL}^c)_p (\psi_{jL})_m (\phi)_n \\ &\quad + h_{1i}^d \bar{Q}_{1L} \phi d_{iR} + h_{\alpha i}^d \bar{Q}_{\alpha L} \phi^* u_{iR} + h.c., \end{aligned} \quad (8)$$

$$\begin{aligned} \mathcal{L}_Y^{\text{mix}} &= h_{1i}^u \bar{Q}_{1L} \chi u_{iR} + h_{\alpha i}^u \bar{Q}_{\alpha L} \chi^* d_{iR} \\ &\quad + h_{1\alpha}'' \bar{Q}_{1L} \phi D_{\alpha R} + h_{\alpha 1}'' \bar{Q}_{\alpha L} \phi^* U_R + h.c. \end{aligned} \quad (9)$$

The VEV ω gives mass for the exotic quarks U , D_α and the new gauge bosons Z' , X , Y , while the VEVs u and v give mass for the quarks u_a , d_a , the leptons l_a and all the ordinary gauge bosons Z , W . To keep a consistency with the effective theory, the VEVs in this model have to satisfy the constraint

$$u^2 \ll v^2 \ll \omega^2. \quad (10)$$

In this model, the most general Higgs potential has very simple form

$$V(\chi, \phi) = \mu_1^2 \chi^\dagger \chi + \mu_2^2 \phi^\dagger \phi + \lambda_1 (\chi^\dagger \chi)^2 + \lambda_2 (\phi^\dagger \phi)^2 + \lambda_3 (\chi^\dagger \chi)(\phi^\dagger \phi) + \lambda_4 (\chi^\dagger \phi)(\phi^\dagger \chi). \quad (11)$$

Note that there is no trilinear scalar coupling and this makes the Higgs potential much simpler than those in the 331RN3HT [3] and closer to that of the SM. The analysis in Ref.[17] shows that after symmetry breaking, there are eight Goldstone bosons and four physical scalar fields. One of two physical neutral scalars is the SM Higgs boson. In the pseudoscalar sector, there are two neutral physical fields-the SM H^0 and the new H_1^0 with masses.

$$M_{H^0}^2 \simeq \frac{4\lambda_1\lambda_2 - \lambda_3^2}{2\lambda_1} v^2, \quad (12)$$

$$M_{H_1^0}^2 \simeq 2\lambda_1 \omega^2. \quad (13)$$

From Eq.(13), it follows that mass of the new Higgs boson $M_{H_1^0}$ is related to mass of the bilepton gauge X^0 (or Y^\pm via the law of Pythagoras) through

$$\begin{aligned} M_{H_1^0}^2 &= \frac{8\lambda_1}{g^2} M_X^2 \left[1 + \mathcal{O}\left(\frac{M_W^2}{M_X^2}\right) \right] \\ &= \frac{2\lambda_1 s_W^2}{\pi\alpha} M_X^2 \left[1 + \mathcal{O}\left(\frac{M_W^2}{M_X^2}\right) \right] \approx 18.8\lambda_1 M_X^2. \end{aligned} \quad (14)$$

Here, we have used $\alpha = \frac{1}{128}$ and $s_W^2 = 0.231$.

In the charged Higgs sector, there are two charged Higgs bosons H_2^\pm with mass

$$\begin{aligned} M_{H_2^\pm}^2 &= \frac{\lambda_4}{2} (u^2 + v^2 + \omega^2) = 2\lambda_4 \frac{M_Y^2}{g^2} \\ &= \frac{s_W^2 \lambda_4}{2\pi\alpha} M_Y^2 \simeq 4.7\lambda_4 M_Y^2. \end{aligned} \quad (15)$$

From Eq. (14) we see that the masses of the new neutral Higgs boson H_1^0 and the neutral non-Hermitian bilepton X^0 are dependent on a coefficient of Higgs self-coupling (λ_1). Eq.(15) gives us a connection between mass of H_2^\pm and bilepton mass Y through the coefficient of Higgs self-coupling λ_4 . Note that in the considered model. To keep the smallness of these couplings, the mass $M_{H_2^\pm}$ can be taken in the electroweak scale with $\lambda_4 \sim 0.01$ [18]. From (15), taking the lower limit for M_Y to be 1 TeV, the mass of H_2^\pm is in range of 200 GeV. Interactions among the standard model gauge bosons and Higgs bosons were studied in detail [11]. From these couplings, all scalar fields including the neutral scalar H^0 and the Goldstone bosons were identified and their couplings with the usual gauge bosons such as the photon, the charged bosons W^\pm and the neutral Z , and also Z' without any additional condition were recovered. Note that The CP-odd part of Goldstone associated with the neutral non-Hermitian bilepton gauge boson G_{X^0} is decouple, while its CP-even counterpart has the mixing by the same way in the gauge boson sector.

III. PAIR PRODUCTION OF H_2^\pm IN e^+e^- COLLIDERS

High energy e^+e^- colliders have been essential instruments to search for the fundamental constituents of matter and their interactions. The possibility to detect the neutral Higgs boson in the minimal version at e^+e^- colliders was considered in [15] and production of the SM-like neutral Higgs boson at the CERN LHC was studied in Ref.[16]. This section is devoted to pair production of H_2^\pm at e^+e^- colliders with the center-of-mass energy is chosen in range between 500GeV (ILC) and 1000GeV . The trilinear couplings of H_2^\pm with the neutral gauge bosons in the SM are given in Table I [11]

From Table I. we can see that pair production of H_2^\pm in e^+e^- colliders exists through the neutral gauge bosons in the SM. Now we consider the process in which the initial state contains the electron and the positron and in the final state there are the pair H_2^\pm

$$e^-(p_1) + e^+(p_2) \rightarrow H_2^+(k_1) + H_2^-(k_2), \quad (16)$$

TABLE I: The trilinear couplings of the pair H_2^\pm with the neutral gauge bosons in the SM.

Vertex	$A^\mu H_2^- \overleftrightarrow{\partial}_\mu H_2^+$	$Z^\mu H_2^- \overleftrightarrow{\partial}_\mu H_2^+$
Coupling	ie	$-igs_W t_W$

The straightforward calculation yields the following differential cross section (DCS) in the center-of-mass frame with the polarized e^+, e^- beams is

$$\frac{d\sigma_{(P_+, P_-)}}{d\cos\theta} = \left(\frac{K_{H_2^+ H_2^-}^3 \pi \alpha^2}{4s^2} \right) \left[\frac{1}{s^2} (1 - P_+ P_-) - \frac{g_z [v_e (1 - P_+ P_-) - a_e (P_- - P_+)]}{2C_W S_W s (s - m_Z^2)} \right. \\ \left. + \frac{g_z^2 [(v_e^2 + a_e^2)(1 - P_- P_+) - 2v_e v_a (P_- - P_+)]}{16C_W^2 S_W^2 (s - m_Z^2)^2} \right] (1 - \cos^2\theta), \quad (17)$$

where θ is angle between \vec{p}_1 and \vec{k}_1 , $g = \frac{e}{s_W}$; $g_Z = \frac{1}{2S_W C_W (\omega^2 + v^2)} (2\omega^2 S_W^2 - v^2 (4C_W^2 - 1))$; $v_e = -1 + 4s_W^2$; $a_e = -1$, and

$$K_{H_2^+ H_2^-} = \left[(s - m_{H_2^+}^2 - m_{H_2^-}^2)^2 - 4m_{H_2^+}^2 m_{H_2^-}^2 \right]^{1/2}. \quad (18)$$

P_+ and P_- are polarized coefficients of e^+ and e^- beams, respectively. The total cross section is given by

$$\sigma_{(P_+, P_-)} = \left(\frac{K_{H_2^+ H_2^-}^3 \pi \alpha^2}{3s^2} \right) \left[\frac{1}{s^2} (1 - P_+ P_-) - \frac{g_z [v_e (1 - P_+ P_-) - a_e (P_- - P_+)]}{2C_W S_W s (s - m_Z^2)} \right. \\ \left. + \frac{g_z^2 [(v_e^2 + a_e^2)(1 - P_- P_+) - 2v_e v_a (P_- - P_+)]}{16C_W^2 S_W^2 (s - m_Z^2)^2} \right], \quad (19)$$

here we take $m_Z = 91.1882 \text{ GeV}$, $v = 246 \text{ GeV}$, $\omega = 1 \text{ TeV}$ and $m_H = 200 \text{ GeV}$ [4].

TABLE II: Number of events with the integrated luminosity of 500 fb^{-1} and $m_H = 200 \text{ GeV}$

\sqrt{s} (GeV)	500	750	1000
$\sigma_{(P_+, P_-)} \text{ (pbarn)}$	8.7×10^{-2}	7.4×10^{-2}	6.1×10^{-2}
Number of events	4350	3700	3050

In Fig.1 we have plotted the cross section $\sigma_{(P_+, P_-)}$ as a function of the P_+ and P_- . The collision energy is taken to be $\sqrt{s} = 1 \text{ TeV}$, and the Higgs mass $m_{H_2^\pm} = 200 \text{ GeV}$. The figure shows that the cross section gets a maximum value as $\sigma_{(P_+, P_-)} = 6 \times 10^{-2} \text{ pbarn}$ for $P_- = -1$ and $P_+ = 1$, while $\sigma_0 = 2.1 \times 10^{-2} \text{ pbarn}$ for $P_- = P_+ = 0$. The DCS as function of $\cos\theta$ is shown in Fig.2, the curve 1 for $P_- = P_+ = 0$ and the curve 2 for $P_- = -1, P_+ = 1$. From Fig.2 we can see that the DCS gets a maximum value at $\cos\theta = 0$, which is similar to the process $e^+ e^- \rightarrow Zh$ in the SM (while the DCS of the reactions $e^+ e^- \rightarrow ZZ, ZA$ gets the minimal value at $\cos\theta = 0$) [9]. The cross section with highly polarized e^+, e^- beams is much larger than those with non-polarized e^+, e^- beams. Following, the dependence of the total cross-section on Higgs mass for the fixed collision energies, typically $\sqrt{s} = 0.5 \text{ TeV}$, $\sqrt{s} = 0.75 \text{ TeV}$ and $\sqrt{s} = 1 \text{ TeV}$, is also shown in Fig. 3 for $P_- = -1, P_+ = 1$ and in Fig. 4 for $P_- = P_+ = 0$. The Higgs mass is chosen as $200 \text{ GeV} \leq m_H \leq 500 \text{ GeV}$. As we can see from the figures, at high energies, the m_H increases then the cross-section decreases, which is equal to zero at $m_H \simeq 500 \text{ GeV}$ for $\sqrt{s} = 1 \text{ TeV}$, at $m_H \simeq 440 \text{ GeV}$ for $\sqrt{s} = \sqrt{0.75} \text{ TeV}$, and at $m_H \simeq 350 \text{ GeV}$ for $\sqrt{s} = \sqrt{0.5} \text{ TeV}$. It is worth noting that there is no difference between two lines at $m_H \simeq 230 \text{ GeV}$, $m_H \simeq 250 \text{ GeV}$ and $m_H \simeq 300 \text{ GeV}$. Taking the integrated luminosity of 500 fb^{-1} [8], Higgs mass is chosen at the relatively low value of 200 GeV , the number of events with different values of \sqrt{s} is

given in Table II. From the results, it shows that with high integrated luminosity and at high degree of polarization of electron and positron beams then the production cross section may give observable values at moderately high energies. The number of events can be several thousand as expected.

IV. PRODUCTION OF $H_2^- W^+$ VIA ZZ' FUSION AT e^+e^- COLLIDERS

The similarity as section III, in this section we examine the pair production of $H_2^- W^+$ at e^+e^- colliders via $Z Z'$ exchange. The trilinear couplings of the pair $H_2^- W^+$ with the neutral gauge bosons in the economical 3-3-1 model are given by[11]

TABLE III: The trilinear couplings of the pair $H_2^- W^+$ with the neutral gauge bosons in the economical 3-3-1 model

Vertex	$Z^\mu H_2^- \partial_\mu W^+$	$Z'^\mu H_2^- \partial_\mu W^+$
Coupling	$\frac{g^2 v \omega}{2\sqrt{\omega^2 + c_\theta^2 v^2}} [s_\theta c_\theta (u_{12} + \sqrt{3}u_{22}) + c_{2\theta} u_{42}]$	$\frac{g^2 v \omega}{2\sqrt{\omega^2 + c_\theta^2 v^2}} [s_\theta c_\theta (u_{13} + \sqrt{3}u_{23}) + c_{2\theta} u_{43}]$

Here $U_{\alpha\beta}$ ($\alpha, \beta = 1, 2, 3, 4$) is a mixing matrix of neutral gauge bosons given in appendix A. The angle θ is a mixing angle between charged gauge bosons W and Y , which is defined by [4]

$$\tan \theta = \frac{u}{\omega}. \quad (20)$$

The decay of charged gauge boson W into leptons and quarks was analyzed in detail in [4], which gives us a upper limit: $\sin \theta \leq 0.08$. From Table II. we can see that pair production of $H_2^- W^+$ in e^+e^- colliders exists through the neutral gauge bosons Z and Z' in the s -channel

$$e^-(p_1) + e^+(p_2) \rightarrow H_2^-(k_1) + W^+(k_2), \quad (21)$$

In this case the DCS is given by

$$\begin{aligned} \frac{d\sigma_{(P_+, P_-)}}{d\cos\theta} = & \left(\frac{K_{H_2^- W^+} \pi^2 \alpha^3}{2s^2} \right) \left\{ \frac{e_Z^2 [(v_e^2 + a_e^2)(1 - P_- P_+) - 2v_e a_e (P_- - P_+)]}{16C_W^2 S_W^2 (s - m_Z)^2} \right. \\ & + \frac{e_Z'^2 [(v_e'^2 + a_e'^2)(1 - P_- P_+) - 2v_e' a_e' (P_- - P_+)]}{16C_W^2 S_W^2 (s - m_{Z'})^2} \\ & \left. + \frac{e_Z e_Z' [(v_e v_e' + a_e a_e')(1 - P_- P_+) - (v_e a_e' + v_e' a_e)(P_- - P_+)]}{8C_W^2 S_W^2 (s - m_Z^2)(s - m_{Z'}^2)} \right\} \left\{ -2s + \frac{K_{H_2^- W^+}^2}{2m_W^2} (1 - \cos^2 \theta) \right\}, \quad (22) \end{aligned}$$

and the total cross-section is

$$\begin{aligned} \sigma_{(P_+, P_-)} = & \left(\frac{K_{H_2^- W^+} \pi^2 \alpha^3}{2s^2} \right) \left\{ \frac{e_Z^2 [(v_e^2 + a_e^2)(1 - P_- P_+) - 2v_e a_e (P_- - P_+)]}{16C_W^2 S_W^2 (s - m_Z)^2} \right. \\ & + \frac{e_Z'^2 [(v_e'^2 + a_e'^2)(1 - P_- P_+) - 2v_e' a_e' (P_- - P_+)]}{16C_W^2 S_W^2 (s - m_{Z'})^2} \\ & \left. + \frac{e_Z e_Z' [(v_e v_e' + a_e a_e')(1 - P_- P_+) - (v_e a_e' + v_e' a_e)(P_- - P_+)]}{8C_W^2 S_W^2 (s - m_Z^2)(s - m_{Z'}^2)} \right\} \left\{ -4s + \frac{2 K_{H_2^- W^+}^2}{3 m_W^2} \right\}, \quad (23) \end{aligned}$$

where $v_e = -1 + 4S_W^2$, $a_e = -1$, $v_e' = \frac{v_e}{\sqrt{4C_W^2 - 1}}$, $a_e' = \frac{a_e}{\sqrt{4C_W^2 - 1}}$,

$$e_Z = \frac{v\omega}{2S_W^2 \sqrt{\omega^2 + C_\theta^2 v^2}} [S_\theta C_\theta (u_{12} + \sqrt{3}u_{22}) + C_\theta^2 u_{42}], \quad (24)$$

$$e'_Z = \frac{v\omega}{2S_W^2\sqrt{\omega^2 + C_\theta^2 v^2}} \left[S_\theta C_\theta (u_{13} + \sqrt{3}u_{23}) + C_{2\theta} u_{43} \right], \quad (25)$$

and

$$K_{H^-W^+} = \left[(s - m_{H_2^-}^2 - m_W^2)^2 - 4m_{H_2^-}^2 m_W^2 \right]^{1/2}. \quad (26)$$

Here we use data as in previous item and $m_{Z'} = 800 \text{ GeV}$ [12]. For the sake of convenience in calculations, we take the upper value of the mixing angle $(s_\theta)_{max} = 0.08$.

In Fig.5 we have plotted the total cross-section $\sigma_{(P_+, P_-)}$ as a function of the polarized coefficients with $P_-, P_+ \in [-1, 1]$. The total cross-section $\sigma_{(P_+, P_-)}$ increases when P_- comes to -1, P_+ comes to +1 and it gets a maximum value by $\sigma_{(P_+, P_-)} = 2.65 \times 10^{-6} \text{ pbarn}$ for $P_- = -1$ and $P_+ = 1$, while the e^+, e^- beams are not polarized then the total cross-section as $\sigma_0 = 0.8 \times 10^{-6} \text{ pbarn}$. The DCS as function of $\cos\theta$ at the fixed energy, typically $\sqrt{s} = 1 \text{ TeV}$, is shown in Fig.6. The curve 1 with $P_- = P_+ = 0$ and the curve 2 with $P_- = -1, P_+ = 1$. From Fig.6 we can see the behavior of DCS is similar as in Fig. 2. The Higgs mass dependence of the total cross-section for the fixed energies as in previous item are shown in the figures, Fig.7 for $P_- = -1, P_+ = 1$ and Fig. 8 for $P_- = P_+ = 0$. The mass range is $200 \text{ GeV} \leq m_H \leq 800 \text{ GeV}$. As we can see from the figures, the total cross-section decreases rapidly as m_H increases. In Fig.9 we have plotted the Higgs mass dependences of the total cross-section at the fixed higher energies, $\sqrt{s} = 1 \text{ TeV}$, $\sqrt{s} = 1.5 \text{ TeV}$ and $\sqrt{s} = 2 \text{ TeV}$. From Fig.9 we can see that at high values of \sqrt{s} , the total cross-section decreases slowly, while at lower energy ($\sqrt{s} = 1 \text{ TeV}$) the total cross-section decreases rapidly as m_H increases and there is no difference between three lines at $m_H \simeq 750 \text{ GeV}$. Based on the results, it shows that the cross-section of pair $H_2^- W^+$ is much smaller than those of pair production H_2^\pm in the same condition. *We deduce that the direct production of $H_2^- W^+$ is in general not expected to lead to easily observable signals in $e^+ e^-$ collisions.*

In the final state, H_2^- can decay with modes as follows

$$\begin{aligned} H_2^- &\rightarrow l\nu_l, \quad \tilde{U}d_a, \quad D_\alpha \tilde{u}_a, \\ &\searrow ZW^-, \quad Z'W^-, \quad XW^-, \quad ZY^-. \end{aligned} \quad (27)$$

Note that in the effective approximation H_2^- is a bilepton. Assuming that masses of the exotic quarks (U, D_α) are larger than $M_{H_2^\pm}$, we come to the fact that, the hadron modes are absent in decay of the charged Higgs boson. Due to that the Yukawa couplings of $H_2^\pm l^\mp \nu$ are very small, the main decay modes of the H_2^\pm are in the second line of (27). Because of the exotic X, Y, Z' gauge bosons are heavy, the coupling of a singly-charged Higgs boson (H_2^\pm) with the weak gauge bosons, $H_2^\pm W^\mp Z$, may be main. For more details, the readers can see in our early work [11]

V. CONCLUSIONS

In conclusion we have presented the economical 3-3-1 model. In this model we have focused attention to the singly-charged Higgs boson with mass is estimated in range of few hundred GeV . Pair production of H_2^\pm in high energy $e^+ e^-$ colliders with polarization of e^+, e^- beams was studied in detail. Numerical evaluation shows that if the mass of them is not too heavy and at high degree of polarization then the production cross section may give observable values at moderately high energies. With the high integrated luminosity $L = 500 \text{ fb}^{-1}$, the number of events can be several thousand as expected. We have considered pair production of $H_2^- W^+$ at high energy $e^+ e^-$ colliders. From our results, it shows that cross-sections for their production at high energies are very small, much below production cross sections of H_2^\pm , so that the direct production of $H_2^- W^+$ is in general not expected to lead to easily observable signals in $e^+ e^-$ annihilation.

Finally, we emphasize that the electron-positron linear collider in the energy range between 500 GeV and 1000 GeV is very important to precisely test the SM and to explore the physics beyond it.

Acknowledgments

One of the authors (D. V. Soa) expresses sincere gratitude to the European Organization for Nuclear Research (CERN) for the financial support. He is also grateful to Prof. J. Ellis for the hospitality during his stay at CERN.

This work was supported in part by National Council for Natural Sciences of Vietnam.

APPENDIX A: MIXING MATRIX OF NEUTRAL GAUGE BOSONS

For the sake of convenience in practical calculations, we used the mixing matrix

$$\begin{pmatrix} W_3 \\ W_8 \\ B \\ W_4 \end{pmatrix} = U \begin{pmatrix} A \\ Z^1 \\ Z^2 \\ W'_4 \end{pmatrix}, \quad (A1)$$

where

$$U = \begin{pmatrix} s_W & c_\varphi C_{\theta'} C_W & s_\varphi C_{\theta'} C_W & s_{\theta'} C_W \\ -\frac{s_W}{\sqrt{3}} & \frac{c_\varphi(s_W^2 - 3c_W^2 s_{\theta'}^2) - s_\varphi \sqrt{(1-4s_{\theta'}^2 c_W^2)(4c_W^2 - 1)}}{\sqrt{3} c_W c_{\theta'}} & \frac{s_\varphi(s_W^2 - 3c_W^2 s_{\theta'}^2) + c_\varphi \sqrt{(1-4s_{\theta'}^2 c_W^2)(4c_W^2 - 1)}}{\sqrt{3} c_W c_{\theta'}} & \sqrt{3} s_{\theta'} C_W \\ \frac{\sqrt{4c_W^2 - 1}}{\sqrt{3}} & -\frac{t_W(c_\varphi \sqrt{4c_W^2 - 1} + s_\varphi \sqrt{1-4s_{\theta'}^2 c_W^2})}{\sqrt{3} c_{\theta'}} & -\frac{t_W(s_\varphi \sqrt{4c_W^2 - 1} - c_\varphi \sqrt{1-4s_{\theta'}^2 c_W^2})}{\sqrt{3} c_{\theta'}} & 0 \\ 0 & -t_{\theta'}(c_\varphi \sqrt{1-4s_{\theta'}^2 c_W^2} - s_\varphi \sqrt{4c_W^2 - 1}) & -t_{\theta'}(s_\varphi \sqrt{1-4s_{\theta'}^2 c_W^2} + c_\varphi \sqrt{4c_W^2 - 1}) & \sqrt{1-4s_{\theta'}^2 c_W^2} \end{pmatrix}.$$

Here we have denoted $s_{\theta'} = \frac{t_{2\theta}}{c_W \sqrt{1+4t_{2\theta}^2}}$. In approximation, the angle φ has to be very small [4]

$$t_{2\varphi} \simeq -\frac{\sqrt{3-4s_W^2}[v^2 + (11-14s_W^2)u^2]}{2c_W^4 \omega^2}. \quad (A2)$$

-
- [1] SuperK, Y. Fukuda *et al.*, Phys. Rev. Lett. **81**, 1562 (1998); **82**, 2644 (1999); **85**, 3999 (2000); **86**, 5651 (2001); Y. Suzuki, Nucl. Phys. B (Proc. Suppl.) **77**, 35 (1999); SuperK, Y. Fukuda *et al.*, Phys. Rev. Lett. **81**, 1158 (1998); **82**, 1810 (1999); Y. Suzuki, Nucl. Phys. B (Proc. Suppl.) **77**, 35 (1999); S. Fukuda *et al.*, Phys. Rev. Lett. **86**, 5651 (2001).
 - [2] F. Pisano and V. Pleitez, Phys. Rev. D **46**, 410 (1992); P. H. Frampton, Phys. Rev. Lett. **69**, 2889 (1992); R. Foot *et al.*, Phys. Rev. D **47**, 4158 (1993).
 - [3] R. Foot, H. N. Long and Tuan A. Tran, Phys. Rev. D **50**, R34 (1994); J. C. Montero, F. Pisano and V. Pleitez, Phys. Rev. D **47**, 2918 (1993); H. N. Long, Phys. Rev. D **54**, 4691 (1996); H. N. Long, Phys. Rev. D **53**, 437 (1996).
 - [4] P. V. Dong, H. N. Long, D. T. Nhung and D. V. Soa, Phys. Rev. D **73**, 035004 (2006).
 - [5] For a review on the Higgs sector in the SM, see J. F. Gunion, H. E. Haber, G. L. Kane, S. Dawson: *The Higgs Hunter's Guide*, Addison-Wesley, Reading 1990.
 - [6] V. A. Ilyin, A. E. Pukhov, Y. Kurihara, Y. Shimizu, T. Kaneko, Phys. Rev. D **54**, 6717 (1996); A. Djouadi, H. E. Haber, P. M. Zerwas, Phys. Lett. B **375**, 203 (1996); F. Boudjema, E. Chopin, Z. Phys. C **73**, 85 (1996).
 - [7] S. Dawson, A. Dittmaier, M. Spira, Phys. Rev. **58**, 115012 (1998).
 - [8] C. A. Baez *et al.*, acta physica slovac, vol.56 No.4, 455 (2006); Chong-Xing Yue, Lei Wang and Li-Na Wang, Chin. Phys. Lett. **23**, 2379 (2006); P. Garcia-Abia, W. Lohmann, and A. R. Raspeza, Eur. Phys. C **44**, 481 (2005).
 - [9] E. Accomando *et al.*, Phys. Rept. **299**, 1-78 (1998).
 - [10] G. Jikia, Nucl. Phys. B **412**, 57 (1994).
 - [11] P. V. Dong, H. N. Long and D. V. Soa, Phys. Rev. D **73**, 075005 (2006).
 - [12] H. N. Long, D. V. Soa, Nucl. Phys. B **601**, 361 (2001);
 - [13] D. V. Soa, Takeo Inami and H. N. Long, Eur. Phys. J. C **34**, 285 (2004).
 - [14] S. Godfrey, P. Kalyniak and N. Romanenko, Phys. Lett. B **545**, 361 (2002).
 - [15] J. E. Cienza Montalvo and M. D. Tonasse, Phys. Rev. D **71**, 095015 (2005).
 - [16] L. D. Ninh and H. N. Long, Phys. Rev. D **72**, 075004 (2005).
 - [17] A. Carcamo, R. Martinez and F. Ochoa, Phys. Rev. D **73**, 035007 (2006).
 - [18] D. Chang, W. Y. Keung and P. B. Pal, Phys. Rev. Lett. **61**, 2420 (1988), C. A. de S. Pires and P. S. Rodrigues da Silva, E. Phys. J. C **36**, 397 (2004).

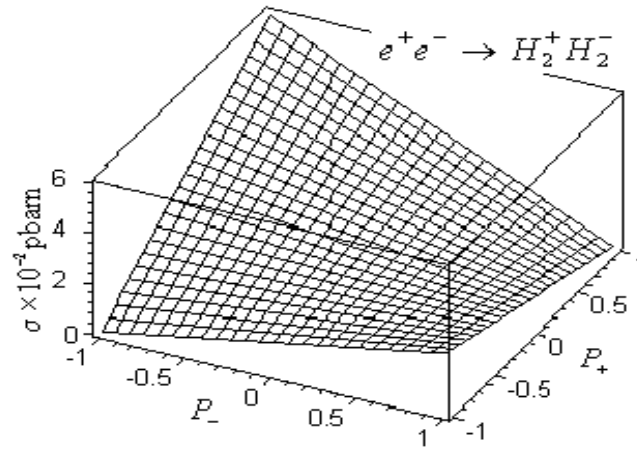


FIG. 1: The total cross-section of the process $e^+e^- \rightarrow H_2^\pm$ as function of polarized coefficients. The collision energy is taken to be $\sqrt{s} = 1 \text{ TeV}$, and Higgs mass $m_{H_2^\pm} = 200 \text{ GeV}$.

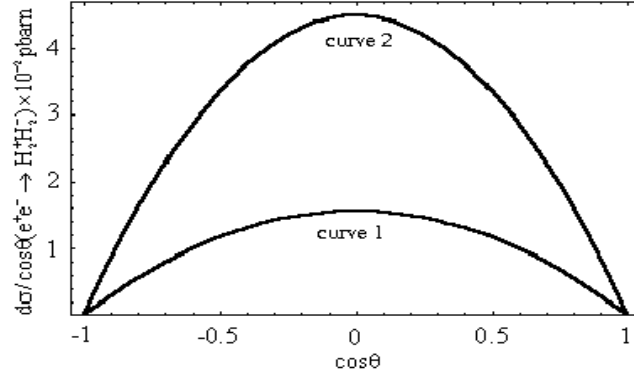


FIG. 2: The DCS of the process $e^+e^- \rightarrow H_2^\pm$ as function of $\cos\theta$. The collision energy is taken to be $\sqrt{s} = 1 \text{ TeV}$, and Higgs mass $m_{H_2^\pm} = 200 \text{ GeV}$. The curve 1 for $P_- = 0, P_+ = 0$, and the curve 2 for $P_- = -1, P_+ = 1$.

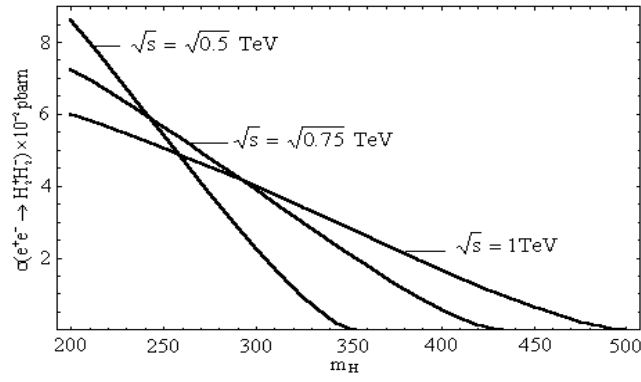


FIG. 3: The total cross-section of the process $e^+e^- \rightarrow H_2^\pm$ as function of m_H for $P_- = -1$ and $P_+ = 1$. The collision energies are taken to be $\sqrt{s} = 0.5 \text{ TeV}$, $\sqrt{s} = 0.75 \text{ TeV}$, and $\sqrt{s} = 1 \text{ TeV}$, respectively.

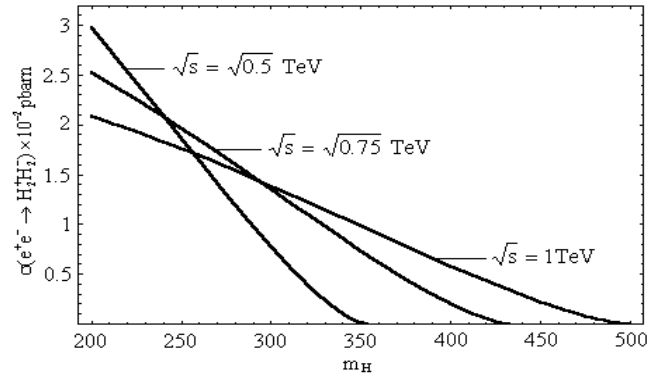


FIG. 4: The total cross-section of the process $e^+e^- \rightarrow H_2^\pm$ as function of m_H for $P_- = P_+ = 0$. The collision energies are taken to be $\sqrt{s} = 0.5\text{TeV}$, $\sqrt{s} = 0.75\text{TeV}$, and $\sqrt{s} = 1\text{TeV}$, respectively.

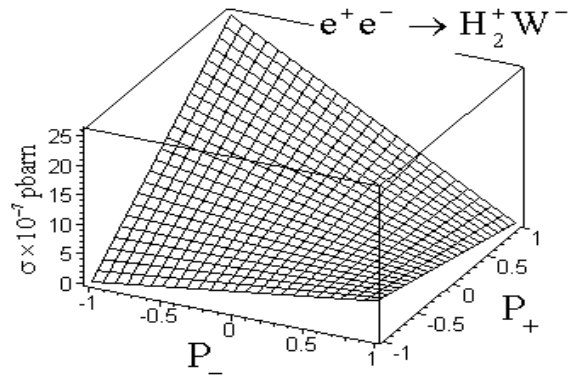


FIG. 5: The total cross-section of the process $e^+e^- \rightarrow H_2^-W^+$ as function of polarization coefficients. The collision energy is taken to be $\sqrt{s} = 1\text{TeV}$, and Higgs mass $m_{H_2^\pm} = 200\text{GeV}$.

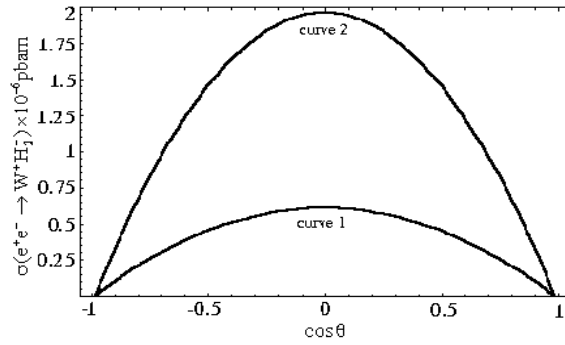


FIG. 6: The DCS as function of the process $e^+e^- \rightarrow H_2^-W^+$ of $\cos\theta$. The collision energy is taken to be $\sqrt{s} = 1\text{TeV}$, and Higgs mass $m_{H_2^\pm} = 200\text{GeV}$. The curve 1 for $P_- = 0, P_+ = 0$, and the curve 2 for $P_- = -1, P_+ = 1$.

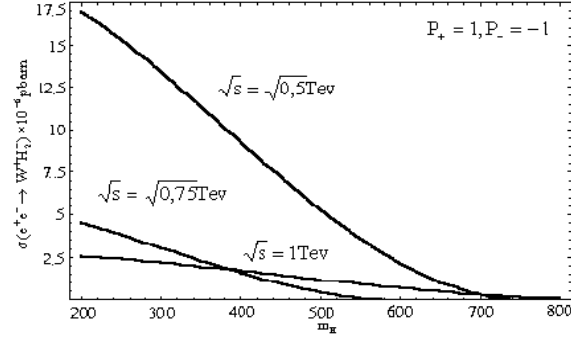


FIG. 7: The total cross-section of the process $e^+e^- \rightarrow H_2^- W^+$ as function of m_H for $P_- = -1, P_+ = 1$. The collision energies are taken to be $\sqrt{s} = 0.5 \text{ TeV}$, $\sqrt{s} = 0.75 \text{ TeV}$, and $\sqrt{s} = 1 \text{ TeV}$, respectively.

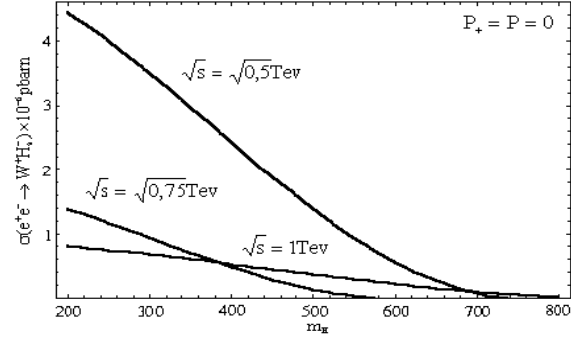


FIG. 8: The total cross-section of the process $e^+e^- \rightarrow H_2^- W^+$ as function of m_H for $P_- = P_+ = 0$. The collision energies are taken to be $\sqrt{s} = 0.5 \text{ TeV}$, $\sqrt{s} = 0.75 \text{ TeV}$, and $\sqrt{s} = 1 \text{ TeV}$, respectively.

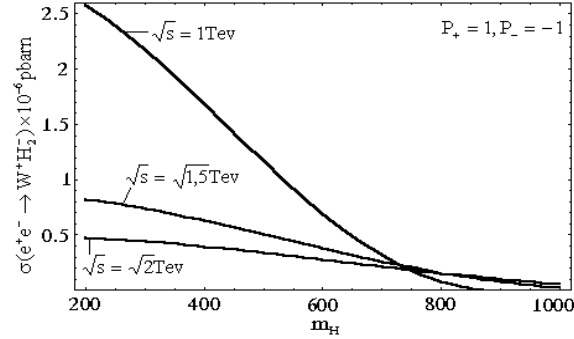


FIG. 9: The total cross-section of the process $e^+e^- \rightarrow H_2^- W^+$ as function of m_H for $P_- = -1, P_+ = 1$. The higher collision energies are taken to be $\sqrt{s} = 1 \text{ TeV}$, $\sqrt{s} = 1.5 \text{ TeV}$, and $\sqrt{s} = 2 \text{ TeV}$, respectively.